# Reversible bistability of conductance on graphene/CuOx/Cu nanojunction

Sangku Kwon, Hyungtak Seo, Hyunsoo Lee, Ki-Joon Jeon, and Jeong Young Park

Citation: Appl. Phys. Lett. **100**, 123101 (2012); doi: 10.1063/1.3694754
View online: http://dx.doi.org/10.1063/1.3694754
View Table of Contents: http://apl.aip.org/resource/1/APPLAB/v100/i12
Published by the American Institute of Physics.

# Reversible bistability of conductance on graphene/$CuO_x$/Cu nanojunction

Sangku Kwon,[1,a)] Hyungtak Seo,[2,a)] Hyunsoo Lee,[1] Ki-Joon Jeon,[3] and Jeong Young Park[1,b)]
[1]*Graduate School of EEWS (WCU), KAIST, Daejeon 305-701, South Korea*
[2]*Department of Materials Science and Engineering, Ajou University, Suwon 443-749, South Korea*
[3]*School of Electrical Engineering, University of Ulsan, Ulsan 680-749, South Korea*

(Received 24 November 2011; accepted 24 February 2012; published online 19 March 2012)

We report that a nanojunction composed of graphene, copper oxide, and Cu substrate exhibits resistive switching behavior, revealed with conductive probe atomic force microscopy at ultrahigh vacuum. The current-voltage curve measured between the titanium nitride-coated tip and the nanojunction exhibited reversible bistable resistance states. We propose that the switching behavior is controlled by the migration of oxygen ions in the copper oxide layer, leading to the reversible formation/disruption of a $CuO_x$-associated charge tunneling barrier, which is consistent with glancing-angle x-ray photoelectron spectroscopy analysis. © *2012 American Institute of Physics*. [http://dx.doi.org/10.1063/1.3694754]

Resistive random access memory (RRAM) is a promising candidate for next generation non-volatile memory (NVM) because it utilizes the bistable resistances of the high-resistance state (HRS) and low-resistance state (LRS) in the materials.[1,2] RRAM has many advantages over future NVM candidates, such as ferroelectric RAM and magnetoresistive RAM, including simple device architecture, low power switching speed, and high density of cells.[3,4] A typical device architecture of RRAM consists of a capacitor-like metal-insulator-metal (MIM) structure. The insulator in MIM functions as a resistive channel operating at the bistable resistance mode. Many binary and complex transition metal (TM) oxides were reported to have resistive switching.[1,5,6] There are two distinguished categories of switching mechanisms in TM oxides: thermochemical and valence changes.[1,7] The thermochemical mechanism is due to the combined effects of local thermal heating and redox reactions that create and control the conductive filaments. Typical switching behavior of the thermochemical mechanism is unipolar switching, as shown in NiO (Ref. 8) and $TiO_2$.[6] The valence change mechanism is caused by the migration of ionic oxygen that leads to changes in electronic conductivity.

Direct experimental observation of the proposed switching mechanisms is a crucial research topic for better understanding and further enhancements of RRAM, but this analysis is challenging because the resistive switching phenomenon stems from local changes in ionic oxygen migration or changes in the conductive filament channel (on the order of nanometers). Recently, visualization of the conductive filament formation has been carried out using high-resolution transmission electron microscope (HR-TEM) studies of the $Ti_4O_7$ RRAM system,[9] providing unique and direct information about the properties of conductive filaments, such as size and density.

In this study, we report the self-aligned formation of a resistive switching device consisting of a graphene/$CuO_x$/Cu stack. The Cu-rich $CuO_x$ channel with resistive switching behavior is created on a Cu substrate by thermal reduction of a native Cu-oxide layer while forming graphene on top of the Cu by chemical vapor deposition (CVD). We detected the migration of ionic oxygen in the $CuO_x$ by measuring the depth profile of $CuO_x$ on each bistable resistance state using glancing-angle x-ray photoelectron spectroscopy (XPS).

The MIM cell was fabricated using the stack of graphene/$CuO_x$/Cu as the top electrode/switching oxide layer/bottom electrode. The Cu-rich $CuO_x$ ($x \sim 0.1$) layer was created by thermal reduction of the Cu surface, which was initially covered with an OH-adsorbed native Cu-oxide layer. This thermal reduction was performed during the graphene synthesis process. The graphene/$CuO_x$ layer was grown by CVD on a copper foil.[10] The substrates were placed in a furnace and heated to 1000 °C under a flow of $H_2$. While still at 1000 °C, a reaction gas mixture ($CH_4$:$H_2$ = 35:0.1 sccm) flowed for 20 min, then the furnace was rapidly cooled to 150 °C.

The resistive switching behavior was measured using a commercial RHK-Tech STM/AFM system mounted in a chamber with a base pressure of $1.0 \times 10^{-10}$ Torr.[11,12] A vacuum is crucial to avoid graphene oxidation and capillary forces between the tip and the sample caused by water at ambient pressure.[13] We used TiN-coated cantilevers, which are conductive and hard with a force constant of 3 N/m (Mikro-Masch). The chemical composition and valence band (VB) edge state of the graphene/Cu nano-junction were analyzed by XPS (Physical Electronics, PHI 5400 ESCA/XPS system equipped with an Al anode x-ray source (1486.6 eV)). The energy resolution for each point is 0.05 eV. All of the peak energy was self-calibrated to C 1s and O 1s reference peak states. Glancing-angle XPS analysis was performed using grazing take-off angles ranging from 10° to 90° between the sample surface normal and the photoelectron analyzer.[14] We applied the bias voltage to change the electrical states before the XPS experiments. The electrodes consist of two parts: the top electrode is in electrical contact with the graphene, and the bottom electrode is in contact with the copper.

[a)]Sangku Kwon and Hyungtak Seo contributed equally to this work.
[b)]Author to whom correspondence should be addressed. Electronic mail: jeongypark@kaist.ac.kr.

 

A scheme of the AFM measurement of the graphene/$CuO_x$/Cu stack is illustrated in Figure 1(a). We carried out conductive AFM to measure I-V curves with nanometer-scale resolution because this measurement allows us to exclude variations in local conductance due to the presence of local disordering and domain structures.[15,16] The stack of graphene/Cu acts as a resistive switching device. Figure 1(b) shows the current-voltage (*I-V*) characteristics measured in the center of a flat region of the graphene/Cu. During the voltage sweep, the I-V curve exhibits a bipolar switching behavior. The ramping speed of the voltage is 9.7 V/s, and the applied load is 35 nN. As we apply a positive voltage greater than the threshold voltage of ~1.5 V, the device switches from LRS to HRS. Switching back from HRS to LRS occurs when a negative voltage was applied below approximately −2.0 V. The statistical distribution of the switching behavior was reported to be typical in $Cu_2O$.[17] Figure 1(c) shows the frequency of the switching bias. It is postulated that this static distribution of switching behavior is due to the energy distribution of the trap level and to the kinetics of the charge trap.[17] The current study suggests that the static distribution of resistive switching at the graphene/Cu junction is also caused by the migration of ionic oxygen, which will be discussed later.

Figure 2(a) shows the XPS spectra of Cu 2p, O 1s, and C 1s binding states on a graphene/$CuO_x$/Cu stack. The elemental XPS peaks were deconvoluted using Gaussian fits. The Cu 2p spectra revealed a major metallic $Cu^0$ peak (the peak areal fraction in Cu 2p > 90%) at 931.9 eV and a weak $Cu^{1+}$ peak (<10%) in $Cu_2O$ at 933.6 eV. In the C 1s XPS spectra, the major peak at 284.5 eV originates from the C-C bond in graphene. Another binding state at 285.7 eV is possibly due to the C-O/C-OH bond formed on the partial defect sites of pristine graphene exposed to air. Corresponding to C and Cu oxidation states, the O 1s spectrum shows O-C (532.2 eV) and O-Cu (529.7 eV) binding states as well as OH groups (531 eV) at the surface. All of these peak assignments coincide with previous XPS studies.[18,19] XPS measurements indicate that a $CuO_x$ ($x \sim 0.1$) layer, composed of a Cu-rich layer, is created by thermal reduction of the Cu surface at ~1000 °C. Once graphene forms, the Cu surface is chemically passivated by the graphene overlayer, with no environmental surface oxidation.[20] In this $CuO_x$ layer, ionic oxygen ($O^{2-}$) can migrate electronically under an external bias, leading to resistive switching.

It is noted from the Cu 2p spectra that native oxide is not dominantly formed on the Cu surfaces. Typically, Cu

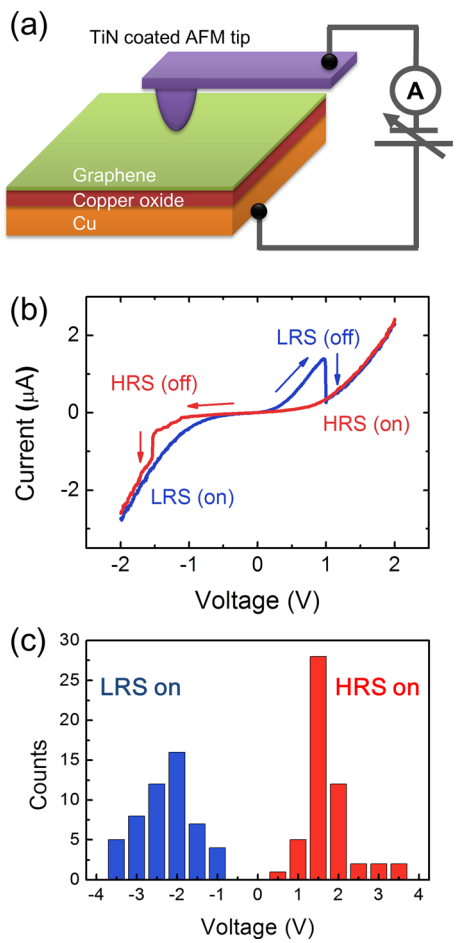


FIG. 1. (Color online) (a) Scheme of the measurement and memristive system that is composed of graphene/Cu with interfacial $CuO_x$. (b) I-V characteristics of the graphene/Cu memristive system that exhibits bipolar switching behavior under the dc voltage sweep. (c) The frequency of switching bias from LRS to HRS and from HRS to LRS.

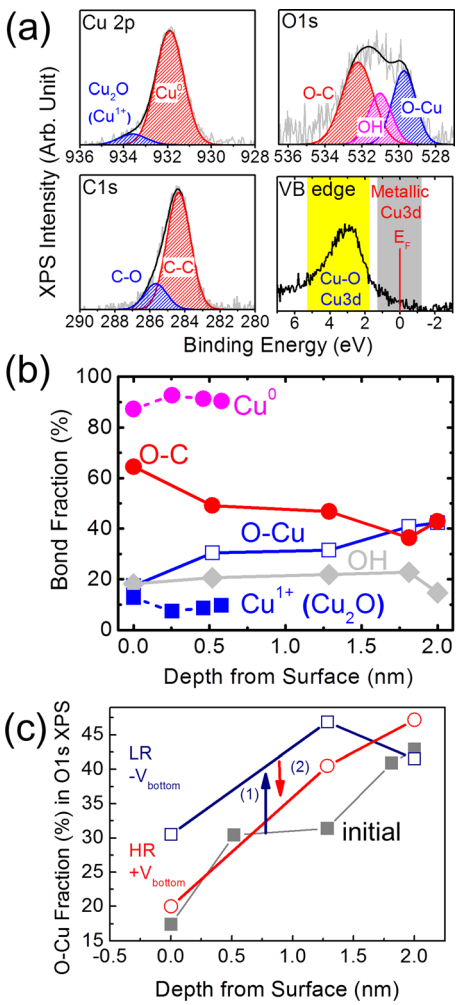


FIG. 2. (Color online) (a) XPS spectra of C 1s, Cu 2p, and O 1s binding states on the graphene/Cu substrate (HRS) at a 50° take-off angle. (b) The depth profile of bond fractions in the graphene/Cu surface region obtained from O 1s spectra for the sample in the HR state. (c) The depth profile of the O-Cu fraction in the graphene/Cu surface region obtained from O 1s spectra for the samples in the initial, HR, and LR states.

surfaces exposed to air suffer from significant native oxide and OH group adsorption, inhibiting observation of the metallic Cu 2p peak in XPS analysis because of the short escape depth of the Cu 2p photoelectron (on the order of ~6 Å).[18] However, in the case of a Cu surface covered with graphene, the two-dimensional, dense, hexagonal network of graphene effectively blocks oxygen diffusion/surface reaction and OH adsorption from the air onto the Cu lattice and preserves the reduced Cu surface. The VB edge spectra in Figure 2(a) indicate that the VB maximum consists of a mixed partial metallic and oxidation state in the Cu 3d and C 2p states of the graphene/$CuO_x$/Cu. The depth profile of the O-Cu fraction in the graphene/Cu surface region has been analyzed by glancing-angle XPS. Figure 2(b) unambiguously reveals a positive gradient of the O-Cu fraction from the top surface (17%) to a depth of ~2 nm (42%) below the Cu surface in a chemical depth profile opposite to the native oxide at the Cu surface. The positive gradient of oxygen in the Cu is consistently found in the Cu 2p depth profile where the Cu-O fraction increases with depth. Therefore, this reinforces that the graphene acts as a buffer layer to prevent environmental oxidation of the Cu surface and, more interestingly, creates a Cu-rich $CuO_x$ phase that enables migration of ionic oxygen.

Figure 2(c) shows a depth profile of the O-Cu fraction obtained from O 1s for three electrical states: initial, LRS, and HRS. The depth profile from the surface was obtained by changing the XPS take-off angle. In the initial state, Cu is relatively rich and oxygen is depleted at the top surface and vice versa deep below the surface, as shown in Figure 2(c). After biasing the bottom electrode from 0 to −2 V, the device switches to the LR state. The negative bias at the bottom electrode leads to the migration of the ionic oxygen in the $CuO_x$ lattice toward the surface. This migration of ionic oxygen is clearly detected in Figure 2(b), showing a 1.5 fold increase of the O-Cu fraction at the top surface, compared to the fresh device. Next, the device was biased from 0 to 2 V and the device switched from the LR to the HR states. In the HR state, ionic oxygen migrates toward the bottom electrode under positive bias. This is also proved by the higher O-Cu fraction deep below the surface, compared to the fresh and LR state devices. The bipolar switching mechanism of the stack is proposed in Figure 3, based on experimental analysis of Figure 2. The correlation between the resistance state switching and the glancing-angle XPS provides an excellent and insightful explanation for the resistive switching mechanism in the graphene/$CuO_x$/Cu device. It is important to note that spectroscopic detection of migrating ionic oxygen in the interfacial $CuO_x$ is possible due to the graphene acting as a chemical buffer layer thin enough for photoelectrons to escape from the Cu surface without significant environmental interfacial oxide formation between the graphene and the Cu. Because of the nature of (1) the high-conductivity channel formed by the Cu-rich $CuO_x$ phase and (2) the low-conductivity channel formed by the oxygen-rich $CuO_x$ phase, the redistribution of oxygen in the graphene/Cu interface is equivalent to the modulation between the conductive channel formation and disruption. Glancing-angle XPS results (Figures 2(b) and 2(c)) suggest that the thickness of the $CuO_x$ layer is greater than 2 nm, which is the maximum

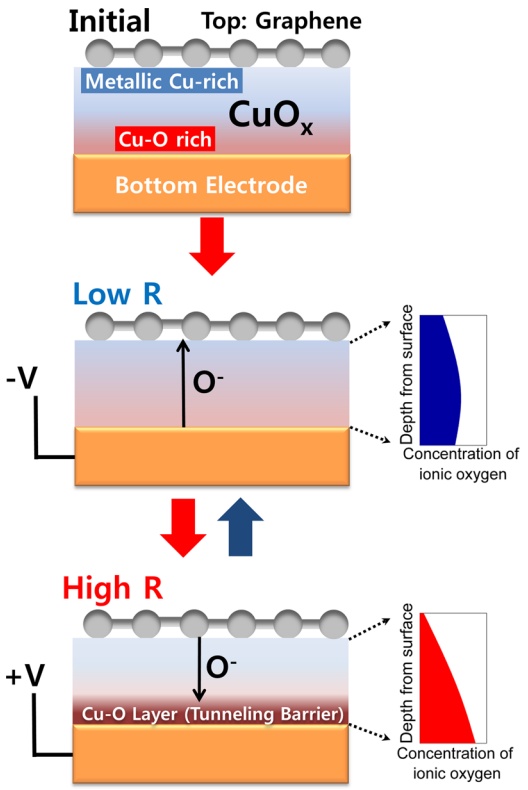


FIG. 3. (Color online) Schematic illustration of the switching mechanism of the graphene/Cu memristive system. The redistribution of ionic oxygen at the graphene/Cu interface driven by migration is equivalent to the modulation between the conductive channel formation (redistribution of ionic oxygen) and disruption (the higher resistive oxygen rich $CuO_x$ formation).

depth limit determined by the mean free path of a photoelectron. The profile of $CuO_x$ at the near-surface region (depth below 2 nm), however, changes in response to the switching bias, as shown in Figure 2(c), which indicates that oxygen ion migration takes place and is responsible for the change of electrical states.

In the thermochemical unipolar switching mechanism, the conductive filament is often described as the local channel aligned with the grain boundary where an oxygen atom has higher diffusivity than in the bulk grain.[21] In this study, XPS analyses suggest a non-local migration of ionic oxygen in the graphene/Cu stack since the spectroscopic analyses, after biasing over a large area (mm scale), reveal noticeable differences in the oxygen fraction in the depth profile. HRS can be regarded due to the two-dimensionally uniform, columnar, oxygen-rich $CuO_x$ phase formations near the bottom electrode that act as a tunneling barrier for the charge injection, as shown in Figure 3.

It should be stressed that the formation of graphene/Cu resistive switching cells can be self-aligned, since the memristive stack forms during the graphene growth process. Another merit of this switching stack is the excellent chemical stability of graphene as an electrode on the switching channel, making reliable oxygen migration in the range of several nm, a much shorter channel length scale than other filament-type oxide channels (e.g., 10 nm). This study not only demonstrates the use of graphene as a chemically inert electrode or diffusion barrier for resistive random access memory, but it also unveils the role of oxygen ion migration

in bipolar switching mechanisms at the ultrathin metallic junction.

In conclusion, reversible bistability of nanoscale conductance was observed on graphene/Cu using conductive probe AFM. The Cu-rich $CuO_x$ channel is fabricated on a Cu substrate using a self-aligned process during graphene synthesis on Cu. The bipolar switching behavior is observed at low switching voltages ($\sim \pm 2$ V). The XPS analysis is consistent with non-local migration of ionic oxygen as an origin for bipolar switching.

The work was supported by the WCU (World Class University) program (Nos. R-31-2008-000-10055-0, KRF-2010-0005390, and KRF-2011-0015387) and the SRC Centre for Topological Matter (Grant No. 2011-0030787) through the National Research Foundation (NRF) of Korea, funded by the Ministry of Education, Science and Technology (MEST) of Korea. This work was also supported by the Excellence Program in the School of Electrical Engineering at the University of Ulsan. H. Seo acknowledges the support from new faculty research fund of Ajou University.

[1]R. Waser, R. Dittmann, G. Staikov, and K. Szot, Adv. Mater. **21**, 2632 (2009).
[2]D. B. Strukov, G. S. Snider, D. R. Stewart, and R. S. Williams, Nature **453**, 80 (2008).
[3]R. Waser and M. Aono, Nature Mater. **6**, 833 (2007).
[4]K. Kim, Microelectron Reliab. **40**, 191 (2000).
[5]K. Szot, W. Speier, G. Bihlmayer, and R. Waser, Nature Mater. **5**, 312 (2006).
[6]B. J. Choi, D. S. Jeong, S. K. Kim, C. Rohde, S. Choi, J. H. Oh, H. J. Kim, C. S. Hwang, K. Szot, R. Waser *et al.*, J. Appl. Phys. **98**, 033715 (2005).
[7]A. Sawa, Mater. Today **11**, 28 (2008).
[8]K. Oka, T. Yanagida, K. Nagashima, T. Kawai, J. S. Kim, and B. H. Park, J. Am. Chem. Soc. **132**, 6634 (2010).
[9]D. H. Kwon, K. M. Kim, J. H. Jang, J. M. Jeon, M. H. Lee, G. H. Kim, X. S. Li, G. S. Park, B. Lee, S. Han *et al.*, Nat. Nanotechnol. **5**, 148 (2010).
[10]K. S. Novoselov, A. K. Geim, S. V. Morozov, D. Jiang, M. I. Katsnelson, I. V. Grigorieva, S. V. Dubonos, and A. A. Firsov, Nature **438**, 197 (2005).
[11]J. Y. Park, D. F. Ogletree, M. Salmeron, C. J. Jenks, and P. A. Thiel, Tribol. Lett. **17**, 629 (2004).
[12]J. Y. Park, D. F. Ogletree, P. A. Thiel, and M. Salmeron, Science **313**, 186 (2006).
[13]S. Kwon, S. Choi, H. J. Chung, H. Yang, S. Seo, S. H. Jhi, and J. Y. Park, Appl. Phys. Lett. **99**, 013110 (2011).
[14]L. Belau, J. Y. Park, T. Liang, H. Seo, and G. A. Somorjai, J. Vac. Sci. Technol. B **27**, 1919 (2009).
[15]J. S. Choi, J. S. Kim, I. S. Byun, D. H. Lee, M. J. Lee, B. H. Park, C. Lee, D. Yoon, H. Cheong, K. H. Lee *et al.*, Science **333**, 607 (2011).
[16]S. Kwon, H. J. Chung, S. Seo, and J. Y. Park, "Domain structures of single layer graphene imaged with conductive probe atomic force microscopy," Surf. Interface Anal. (in press) (2012).
[17]A. Chen, S. Haddad, Y. C. Wu, Z. Lan, T. N. Fang, and S. Kaza, Appl. Phys. Lett. **91**, 123517 (2007).
[18]H. Roulet, G. Dufour, A. Cheenne, F. Rochet, and C. Cartier, Appl. Surf. Sci. **47**, 173 (1991).
[19]T. Yano, M. Ebizuka, S. Shibata, and M. Yamane, J. Electron. Spectrosc. Relat. Phenom. **131**, 133 (2003).
[20]S. S. Chen, L. Brown, M. Levendorf, W. W. Cai, S. Y. Ju, J. Edgeworth, X. S. Li, C. W. Magnuson, A. Velamakanni, R. D. Piner *et al.*, ACS Nano **5**, 1321 (2011).
[21]M. J. Lee, S. Han, S. H. Jeon, B. H. Park, B. S. Kang, S. E. Ahn, K. H. Kim, C. B. Lee, C. J. Kim, I. K. Yoo *et al.*, Nano Lett. **9**, 1476 (2009).